Image Restoration for Spherical Surface Reflections

Stellacore Corporation
Dave Knopp

Document ID: t_Reflect_v0r2p0, 2020-09-29 08:19:17 -0600

***Abstract*—This technical note describes basic ray tracing formulae for a simple cataoptric imaging system comprising a generic perspective imaging camera in combination with a reflective spherical ball. It describes the associated optical ray geometry utilizing the mathematical framework of geometric algebra. Validity of the developed math model is demonstrated by rectifying a real photographic image taken with a smart phone and a mirrored spherical ornament. Although the general results are entirely standard, the treatment contains a touch of novelty within the mathematics of the geometric algebra formulation. Ray reflection is expressed in terms of a spinor-valued quadratic equation that encodes the complete three-dimensional geometry of the reflection operation. Solution of this equation determines the location on the sphere at which a ray, emanating from an arbitrary object point, is reflected toward the imaging camera. Although quadratic in nature, the reflection equation involves non-commutative elements and an analytical solution is not obvious. An effective and efficient numeric solution is presented and demonstrated to work well with actual image data.**

I. Introduction

A simple cataoptric system may be constructed trivially by photographing a spherical reflector using a generic perspective camera system. Figure 1 illustrates this situation in which a holiday ornament acts as the reflective element placed in front of a standard smartphone camera. To be technically correct, the combination illustrated is actually a catadioptric system comprising both mirrored ball and also the refractive camera system optics. However for current purposes, the reflection from the mirror is of primary interest and the reflective cataoptric behavior is emphasized.

This brief technical note describes an exact mathematical description that can be used for reconstruction of object-space ray directions in association with the reflected geometry recorded by the perspective camera.

It is relatively easy to perform the inverse ray trace leaving from the camera system, reflecting from the sphere and continuing into object space and this inverse direction has a simple closed form solution. However, tracing in the forward direction, following the path of physical photon propagation, is not as simple.

The forward ray trace requires determining a point of reflection on the sphere surface that corresponds to an arbitrary (but otherwise known) object point location. The point of reflection must be determined in such a way that the reflected ray propagates directly toward the camera entrance pupil. This forward case is more involved, because the direction of the ray recorded at the camera is also unknown. Tracing in the forward direction is the primary focus herein. However, for completeness, a solution to the inverse problem is presented in appendix B.

Figure 1. Simple reflective optical system comprising perspective camera viewing a reflective spherical ball. The top portion is an image directly recorded by a smartphone camera while pointed toward a front-silvered spherical ornament. The bottom section shows a restored image created with the formulae presented herein. The rendered image is produced by projecting restored ray directions onto a virtual cylindrical screen.

A. Conventions and Notations

This development utilizes the mathematical framework of Geometric Algebra[1] with conventions and notation generally following those of Hestenes [2] including:

- Scalar quantities are represented with lower case greek letters $(\alpha, \beta, \gamma, \dots)$
- Vector quantities are represented with lower case roman letters $(a, b, c, \dots)$
- Bivector and Spinor quantities are represented by upper case Roman letters $(A, B, C, \dots)$
- The magnitude of a vector, x, is denoted as $|x|$, where $|x| = \sqrt{x^2} = \sqrt{x \cdot x}$
- Unit direction associated with any non-zero vector, x, is denoted by $\hat{x}$, where $\hat{x} \equiv \frac{x}{|x|} = \frac{x}{\sqrt{x^2}}$

II. Methodology

A. General Formulation

1) Incidence Plane: The geometry of the incident plane is illustrated in figure 2. Let the plane of incidence be denoted with unitary bivector[2], I, which may be determined in terms of

[1]The Cambridge web site [1] provides a number of introductory materials and links that describe the basic concepts and universal applicability of "Geometric Algebra" to virtually all fields of science and engineering.

[2]Following the consistent notation of upper case Roman letters for bivectors, an uppercase "I" is used here to denote the incidence plane direction. It should not be confused with the notation many authors use for representing a unitary trivector.

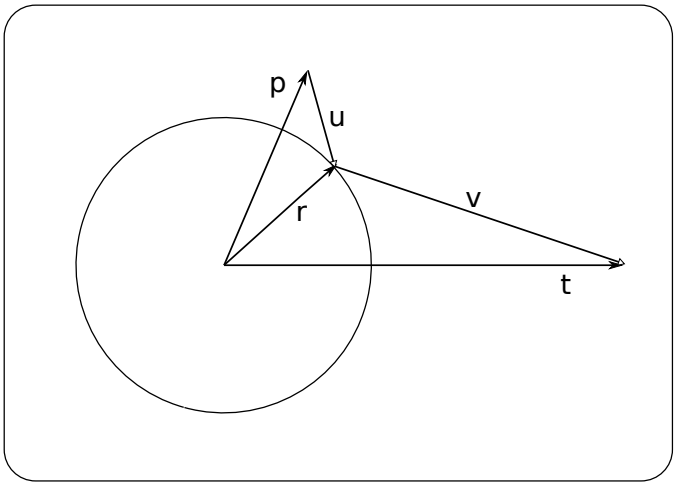

Figure 2. Ray geometry associated with spherical surface. The cross-section figure is drawn in the plane of incidence for an arbitrary individual ray of interest. The incidence plane is determined by three points; the center of the sphere located at the origin, the position of the camera system perspective center (entrance pupil) at vector location, t, and an arbitrary object point of interest at vector location, p. In physical terms, a photon leaving point, p, is incident on the spherical surface at vector location, r, where it is reflected and redirected toward the camera station at t. Vector, $u = r - p$, is aligned to the direction of incidence, and vector, $v = t - r$, is aligned to the direction of reflection.

the camera and object location positions relative to the sphere center at the origin, as

$$I = \frac{t \wedge p}{|t \wedge p|}$$

2) The Sphere: The location on the sphere, associated with scalar radius ρ, is represented by vector, r, with $|r| = \rho$. The point of incidence at location, r, may be expressed in terms of scaling and rotation of the relative camera location, t. Let scalar, α, represent the magnitude of the angle between t and r, such that,

$$r = \rho e^{-\frac{1}{2}I\alpha}\frac{t}{|t|}e^{\frac{1}{2}I\alpha} = \rho\frac{t}{|t|}e^{I\alpha} \tag{1}$$

and

$$\frac{|t|}{\rho}r = te^{I\alpha} \tag{2}$$

3) Reflection Geometry: Let the incident ray be associated with vector, u, defined as

$$u \equiv r - p \tag{3}$$

and the reflected ray be associated with vector, v, defined as

$$v \equiv t - r \tag{4}$$

In terms of unitary directions of the incident ray, $\hat{u} = \frac{u}{|u|}$, and of the reflected ray, $\hat{v} = \frac{v}{|v|}$, the optical law of reflection may be expressed as a geometric reflection through vector, r, or equivalently through the unitary direction, $\hat{r} = \frac{r}{\rho}$, as

$$\hat{v} = -r\hat{u}r^{-1} = -\hat{r}\hat{u}\hat{r} \tag{5}$$

4) External/Internal Reflections: For the expected two solutions, one is expected to be associated with "internal" reflection from the concave interior surface. The second solution may either be an "external" reflection from the convex surface (the one interest here), or the second solution can also represent an internal reflection. The situation in which both solutions represent internal reflections occur when the object point is geometrically occluded by the sphere as viewed from the camera station.

a) Convex Reflection: External reflection from the convex outer surface is associated with the algebraic conditions,

$$r \cdot u < 0$$

and

$$0 < r \cdot v$$

b) Concave Reflection: Internal reflection from the concave inner surface is associated with algebraic conditions,

$$0 < r \cdot u$$

and

$$r \cdot v < 0$$

c) Critical Reflection: The special case in which the incident and reflected rays are tangent to the surface of the sphere is represented by the intermediate conditions,

$$r \cdot u = 0$$
$$r \cdot v = 0$$

Since all three vectors are coplanar, this also implies the reflected and incident rays are parallel, such that,

$$u \wedge v = 0$$

In geometric terms, this situation describes a right circular cone with surface that wraps tangentially around the sphere while having an apex located at the camera perspective center.

5) Reflection Condition: Returning to equation 5, the vector on the left and vector valued product on the right are (anti)parallel. Therefore, the bivector grade of their product vanishes so that the reflection condition may be represented succinctly as,

$$\langle \hat{v}\hat{r}\hat{u}\hat{r} \rangle_2 = 0 \tag{6}$$

This homogeneous relationship is independent of overall scale, and (for non-degenerate configurations) may be expressed as

$$\frac{1}{|v|\,|u|\,|t|^2}\left\langle v\left(\frac{|t|}{\rho}r\right)u\left(\frac{|t|}{\rho}r\right)\right\rangle_2 = 0$$

Assuming all magnitude factors are non-zero, then the overall leading scale factor is unimportant and the bivector factor in brackets must vanish. Substitute relationship 2 to express this as

$$\left\langle v\left(te^{I\alpha}\right)u\left(te^{I\alpha}\right)\right\rangle_2 = 0$$

Note that all vectors lie in the same incidence plane and are parallel with bivector direction, I. Therefore, all of the incidence plane vectors conjugate-commute with the spinor, $e^{I\alpha}$, and the reflection condition may be expressed as,

$$\left\langle vte^{I\alpha}ute^{I\alpha}\right\rangle_2 = \left\langle vtue^{-I\alpha}te^{I\alpha}\right\rangle_2 = \left\langle vtute^{2\alpha I}\right\rangle_2 = 0$$

For later convenience, represent the reflection condition with the negated relationship,

$$\left\langle -vtute^{2\alpha I}\right\rangle_2 = 0 \tag{7}$$

The triple product factor, vtu, can be expanded in terms of r, p, and t, via equations 3 and 4,

$$\begin{aligned} vtu &= (t-r)\,t\,(r-p) \\ &= t^2 r - rtr + rtp - t^2 p \end{aligned}$$

Multiply this from the right by t, to obtain

$$vtut = t^2 rt - rtrt + rtpt - t^2 pt$$

Substitute from equation 1 for r, to obtain,

$$\begin{aligned} vtut &= t^2 \frac{\rho t}{|t|} e^{I\alpha} t - \frac{\rho t}{|t|} e^{I\alpha} t \frac{\rho t}{|t|} e^{I\alpha} t + \frac{\rho t}{|t|} e^{I\alpha} tpt - t^2 pt \\ &= t^2 \frac{\rho t}{|t|} e^{I\alpha} t - \frac{\rho^2}{t^2} t e^{I\alpha} t t e^{I\alpha} t + \frac{\rho t}{|t|} e^{I\alpha} tpt - t^2 pt \\ &= \rho\,|t|\, t e^{I\alpha} t - \rho^2 t e^{2I\alpha} t + \frac{\rho}{|t|} t e^{I\alpha} tpt - t^2 pt \end{aligned}$$

Employ the conjugate-commute relationships once again to yield,

$$\begin{aligned} vtut &= \rho\,|t|\, t t e^{-I\alpha} - \rho^2 t t e^{-2I\alpha} + \frac{\rho}{|t|} t t p t e^{-I\alpha} - t^2 pt \\ &= \rho\,|t|^3\, e^{-I\alpha} - \rho^2\,|t|^2\, e^{-2I\alpha} + \rho\,|t|\, pte^{-I\alpha} - t^2 pt \end{aligned}$$

Lastly, multiply from the right by $-e^{2I\alpha}$, to obtain,

$$-vtute^{2I\alpha} = -\rho\,|t|^3\, e^{I\alpha} + \rho^2\,|t|^2 - \rho\,|t|\, pte^{I\alpha} + t^2 pte^{2I\alpha}$$

Finally, rearrange this, to represent the reflection condition of equation 7 as the bivector condition relationship,

$$\left\langle t^2 pte^{2I\alpha} - \rho\,|t|\left(|t|^2 + pt\right) e^{I\alpha} + \rho^2\,|t|^2 \right\rangle_2 = 0 \tag{8}$$

6) Reflection Equation: This is a quadratic equation in the (non-unitary) spinor, $e^{\alpha I}$. For convenience, introduce (non-unitary) spinor coefficient factors, A, B, and scalar coefficient, γ, defined as

$$A \equiv t^2 pt \tag{9}$$

$$B \equiv -\rho\,|t|\left(|t|^2 + pt\right) \tag{10}$$

$$\gamma \equiv \rho^2\,|t|^2 \tag{11}$$

Use the coefficient parameters to express the reflection quadratic from equation 8 as

$$\left\langle Ae^{2\alpha I} + Be^{\alpha I} + \gamma \right\rangle_2 = 0 \tag{12}$$

The spinor coefficients, A, B, and γ, are determined by knowledge of the camera station location at, t, the object point location at p, and the radius of the sphere, ρ. The unitary bivector direction, I, is completely determined in terms of t and p. Therefore, the reflection condition is (the bivector grade of) a spinor-valued equation quadratic in α. Solution of this equation for scalar values of α, determines the location of the point of reflection at r via relationship 1.

Since scalar coefficient, γ, has zero bivector grade, equation 12 is equivalent to,

$$\left\langle Ae^{2\alpha I} + Be^{\alpha I} \right\rangle_2 = 0 \tag{13}$$

Unfortunately, the grade selection operation complicates the ability to solve this equation algebraically. If the expression inside the angle brackets were known to be zero, then the quadratic could be solved readily (e.g. by completing the square). However, this expression is not zero, but instead is equivalent to some unknown scalar value. I.e. Introduce (unknown) scalar value, σ, to express the reflection relationships in geometric product form as,

$$Ae^{2\alpha I} + Be^{\alpha I} + \gamma = \sigma$$

In this form, both the unknown scalar values, α and σ, must be solved simultaneously in order to determine the point of reflection.

Because both σ and α must be determined, it is not obvious how to proceed with an algebraic solution. However, for general practical applications a simple iterative numeric solution is quite effective. A standard root finding algorithm can be used to determine the solution values of α, which satisfy equation 13. The details of a classic Newton-Raphson technique are described further below. In general, both roots of the quadratic relationship can be recovered from the iterative algorithm by using two distinct, readily distinguishable, approximate starting values.

a) Scaled Coefficients: Since the quadratic equation is homogeneous, all coefficients can be scaled by the same scalar factor (e.g. t^{-2}) without changing the geometric relationship. Potentially useful scaled coefficients include:

$$\begin{aligned} A' &\equiv pt \\ B' &\equiv -\rho\left(|t| + \frac{1}{|t|} pt\right) \\ \gamma' &\equiv \rho^2 \end{aligned}$$

This expresses the coefficients in terms that emphasize the (non-unitary) spinor quantity, pt.

Another expression for the coefficients is in terms that emphasize the relative general angle of p w.r.t. t, in the form of (non-unitary) spinor, pt^{-1}.

$$\begin{aligned} A'' &\equiv pt^{-1} \\ B'' &\equiv -\rho\frac{1}{|t|}\left(1 + pt^{-1}\right) \\ \gamma'' &\equiv \frac{\rho^2}{|t|^2} \end{aligned}$$

For the special case in which the camera is located a unit distance from the sphere center, both of these expressions reduces to

$$\begin{aligned} A' = A'' &= pt \\ B' = B'' &= -\rho\,(1 + pt) \\ \gamma' = \gamma'' &= \rho^2 \end{aligned}$$

B. Numeric Solution

The quadratic equation 12, can be solved effectively with a simple Newton-Raphson iterative numeric technique. This involves determination of a suitable initial value followed by a sequence of iterative refinements that (ideally) converge

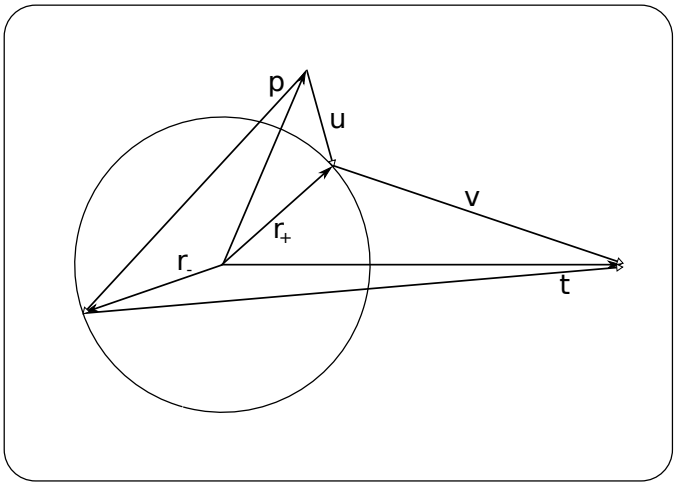

Figure 3. Two geometric solutions for reflection from a spherical surface. One is convex reflection from the outside surface at r_+, and the other is a concave reflection from the inner surface of the sphere at r_-.

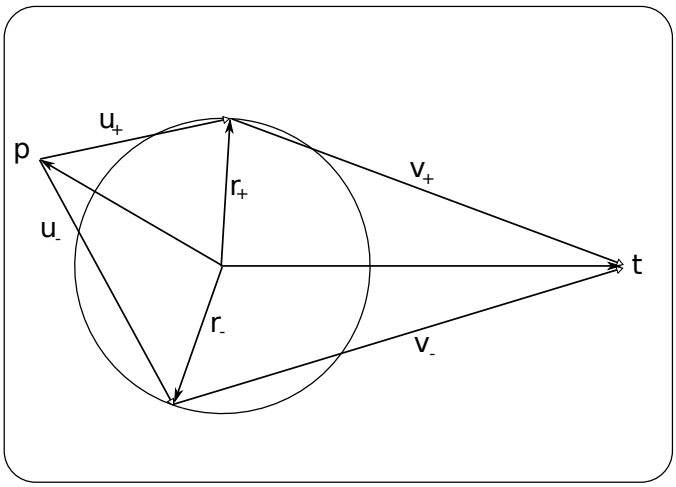

Figure 4. Two internal reflections associated with object point position, p, located "behind" the sphere as viewed from the perspective center position at t.

to the final solution. For the present case, the quadratic relationships involved are relatively smooth and well-behaved such that convergence is generally reliable and quick. This leaves determination of suitable initial values as the remaining step. For the case here, good initial values can be determined easily by inspection of the basic geometry.

Since the reflection condition is represented by a quadratic equation, two solutions are expected. Geometrically these correspond to a convex reflection from the outside surface of the sphere (the desired solution here) and a second solution for concave reflection from the inside of the sphere. From simple geometric intuition, these two solutions can be expected to be distinct and correspond to vector, r, pointing in crudely opposite directions as illustrated in figure 3.

1) Initial Estimate Determination: Denote initial values by a naught subscript. The radius vector, r, is known to have magnitude ρ. Therefore, only the direction, $\hat{r}_0$, needs to be estimated (corresponding to the angle magnitude value α_0).

a) Geometric Average Direction (Mid-Angle): One reasonable starting value for the radius vector, r_0, is to point it at a location half way between the camera and object point directions (as observed from the center of the sphere). I.e. to align r_0 halfway between the directions, $\hat{t}$ and $\hat{p}$.

To express this algebraically, let bivector angle, $\Theta = \vartheta I$, represent the planar angle from direction, $\hat{t}$, into direction $\hat{p}$. This bivector angle may be computed directly from t and p, via

$$\Theta = \ln\left(\hat{t}\hat{p}\right) = \langle \ln\left(tp\right)\rangle_2$$

The initial value, α_0, may then be selected consistent with half of this angle,

$$\alpha_0 I = \frac{1}{2}\Theta = \frac{\vartheta}{2} I$$

The initial angle magnitude can therefore be computed explicitly as,

$$\alpha_0 = -I\frac{1}{2}\ln\left(\hat{t}\hat{p}\right)$$

The reflection vector, r_0, can be computed from this angle magnitude via relationships in equation 1.

Alternatively, r_0 may be expressed directly in terms of t and p by considering the rotation of direction, $\hat{t}$, through the angle $\frac{1}{2}\Theta$, and then scaling by the sphere radius. E.g. combine the preceding relationships to obtain,

$$\alpha_0 I = \frac{1}{2}\ln\left(\hat{t}\hat{p}\right)$$

from which,

$$e^{\alpha_0 I} = \exp\left(\frac{1}{2}\ln\left(\hat{t}\hat{p}\right)\right) = \sqrt{\hat{t}\hat{p}}$$

Insert this into equation 1, in the form,

$$r_0 = \rho\hat{t}e^{\alpha_0 I}$$

leading to

$$r_0 = \rho\hat{t}\sqrt{\hat{t}\hat{p}}$$

This provides an expression for an initial reflection point that bisects the angle between the camera and object point directions and is expressed direction in terms of the camera and object point locations.

To find internal reflections from the concave surfaces, complementary initial values may be determined as

$$\alpha_{0-} = \alpha_0 + \pi$$

or, equivalently with,

$$r_{0-} = -r_0$$

b) Linear Average (Mid-Point): Another convenient starting value for the radius vector, r_0, is to point it toward a location half way between the camera and object point directions (as observed from the center of the sphere). This is particularly suitable when the object distance and camera distances are comparable[3]. E.g.

$$r \propto \frac{1}{2}\left(t + p\right)$$

[3]This is an exact solution for the special case in which the object distance is equal to the camera station distance, (i.e. for $|p| = |t|$).

A good initial value for the reflection point relative to the sphere center is at distance ρ, along this direction, i.e.,

$$r_0 = \rho \frac{t+p}{|t+p|}$$

If the secondary (concave reflection) solution is of interest, a reasonable initial value from which to find the second solution is obtained simply by using the negative of this. Therefore, two useful initial values for the two solutions may be specified as

$$r_{0\pm} = \pm\rho \frac{t+p}{|t+p|}$$

The corresponding initial values for the angle, α_0, can be determined directly by incorporating relationship 1,

$$r_{0\pm} = \rho \frac{t}{|t|} e^{I\alpha_{0\pm}} = \pm\rho \frac{t+p}{|t+p|}$$

Invert this relationship to obtain the initial angle magnitude, α_0, as

$$\alpha_{0\pm} = -I \ln\left(\pm \frac{t}{|t|} \frac{t+p}{|t+p|}\right) \tag{14}$$

The singularity at $p = -t$, is generally of little practical interest since it represents an object point that is occluded by the sphere. However, to be complete, the solution to the reflection point for this special case can be determined by inspection. A valid reflection point, r, can be anywhere on the "equator" of the sphere where the equator is defined relative to the "pole" location toward camera station at t.

2) Linearization: The Newton-Raphson root finding method proceeds in steps wherein each step involves solution of the linear approximation to the equation of interest. To linearize, equation 12, introduce bivector-valued function, F, defined as

$$F(\alpha) = \left\langle Ae^{2\alpha I} + Be^{\alpha I} + \gamma \right\rangle_2$$

For evaluation purposes, the scalar term γ, can be dropped since it does not contribute to the bivector grade. However, it is included here and in the following for algebraic completeness.

Using the linear approximation in the context of reflection condition,

$$\left[F(\alpha) \simeq F(\alpha_0) + \left.\frac{\partial F}{\partial \alpha}\right|_0 (\alpha - \alpha_0)\right] = 0$$

From which

$$\alpha \simeq -\left(\left.\frac{\partial F}{\partial \alpha}\right|_0\right)^{-1} F(\alpha_0) + \alpha_0$$

a) Derivative: Since bivector, I, is constant for the current plane of incidence under consideration, $\frac{\partial}{\partial \alpha} I = 0$, and the derivative of the exponentional term is simply $\frac{\partial}{\partial \alpha} e^{\alpha I} = e^{\alpha I} I$, so that,

$$\frac{\partial F}{\partial \alpha} = \left\langle Ae^{2\alpha I} 2I + Be^{\alpha I} I \right\rangle_2$$

3) Update Formula: The iterative update relationship for computing the $(n+1)$-th value of α, given the angle magnitude, α_n, at the previous iterative step, may be expressed

$$\alpha_{n+1} = \alpha_n - \left(\left.\frac{\partial F}{\partial \alpha}\right|_n\right)^{-1} F(\alpha_n)$$

In terms of the quadratic coefficients, this may be computed via

$$\alpha_{n+1} = \alpha_n - \frac{\left\langle Ae^{2\alpha_n I} + Be^{\alpha_n I} + \gamma \right\rangle_2}{\left\langle \left(2Ae^{2\alpha_n I} + Be^{\alpha_n I}\right) I \right\rangle_2} \tag{15}$$

The fractional representation is justified since the derivative bivector and function bivectors are coplanar and therefore multiplicatively commutative.

4) Convergence Critera: For this simple one-dimensional root finding process, a reasonable, and generally sufficient, process is to continue updating until changes in the evolving angle estimate are inconsequential for the application at hand. I.e. stop the iteration process when the (scalar-valued) update term satisfies

$$\frac{\left\langle Ae^{2\alpha_n I} + Be^{\alpha_n I} + \gamma \right\rangle_2}{\left\langle \left(2Ae^{2\alpha_n I} + Be^{\alpha_n I}\right) I \right\rangle_2} < \epsilon_\alpha \tag{16}$$

for some sufficiently small scalar value, ϵ_α. A typical generic value for ϵ_α, is to use some multiple of machine precision (e.g. $\sqrt{\epsilon_m}$, where ϵ_m is machine precision). However, for many applications, a less demanding value may be appropriate, and the more conservative value may eliminate an iteration or two in the iterative sequence[4].

As an alternative convergence evaluation method, track the position vector at each iteration by computing

$$r_n = \rho \hat{t} e^{I\alpha_n} \tag{17}$$

then stopping the iterative solution process when

$$(r_n - r_{n-1})^2 < \epsilon_r \tag{18}$$

for a sufficiently small (and/or application specific) scalar value, ϵ_r.

Testing convergence directly with the vector location can be particularly appropriate for applications explicitly concerned with the 3D or surface location of the reflection point on the sphere.

5) Solution Recipe: A recipe for the complete numerical solution may be expressed in terms of an iterative process with step index, n:

1) Use the available vectors, t, p, and known sphere radius, ρ, to compute the quadratic equation coefficients, A, B, and γ, using equations 9, 10, and 11.
2) For $n = 0$, determine α_0, directly from t and p, using equation 14 (using the "+" version when interested in a convex reflection solution).

[4]In practice, the effect of reducing the convergence criteria is often small since the process has expected quadratic convergence in any case. For example, it is often typical to reach machine precision in a half dozen iterations or less. However, if the convergence precision can be relaxed by many orders of magnitude, then sometimes the last iteration or possibly the last two might be avoided. Often this is not a practical concern. However, for time critical performance it may be worth considering.

Figure 5. Source image (full frame) used as input for example rectification processing. Acquisition of the image involved nothing special beyond aiming at the ball (and encouraging camera auto-focus to focus on reflected image rather than the surrounding background). Although, here the camera is near the same height as the ball (in actuality, a few centimeters below it), the camera could be held in any position. The rectified image result is "leveled" after the fact by identifying a number of points in the reflected image that should correspond to a local horizon location in a rectified output image.

3) Iterate over integer values of n, for $0 \leq n$, until convergence
   a) Determine α_{n+1} via equation 15
   b) Test for convergence using either equations 16 or 18 as appropriate to application at hand.
4) After convergence, the point of reflection on the spherical surface, r_n, is given by equation 17.
5) Assess the appropriateness of the solution using one of the tests described in sections II-A4a, II-A4b, or II-A4c.

III. Results

To confirm the various formulae presented herein, a simple experiment was conducted with an actual image acquired from a smartphone camera looking into a reflective sphere. Using the ray tracing relationships presented in the preceding sections, the source image was rectified onto the cylindrical surface.

A. Source Image

A standard commercially available smartphone (a Motorola Play 8) was used to photograph an outdoor scene as reflected from a mirrored holiday ornament ball. The source image is shown in figure 5.

B. Rectification Process

The rectification computation process, as employed in this experiment, included the following steps.

1) General System Orientation:: The first steps involve determining the general geometry configuration of the ball, the perspective camera and their alignment with a desired output coordinate frame.

1) Determine the overall geometry. I.e. assign values to critical catadioptric system parameters including the sphere radius, ρ, and the relative camera offset, t.
   a) The spherical ornament in use has a radius, ρ, known from the manufacturer to be 65 millimeters.
   b) The magnitude of the camera standoff distance, $|t|$, is determined from simple trigonometric relationships given the known camera geometry (specifically, $|t| = \frac{\eta}{\delta}\rho$ where η is the camera principal distance and δ is the observed diameter of the image of the sphere). The direction $\hat{t}$, is set identically to coordinate axis basis direction e_3, which is used to defined the principal optical axis of the catadioptric system.
   c) Alignment (attitude) of the camera was determined by fitting a two-dimensional ellipse shape to the edge of the ball image and then using standard geometric relationships to determine the direction to the ball center. Rotation of the camera about this center is left arbitrary (defined by image advancing row direction).
2) The geometry of the perspective camera may be expressed in terms of camera calibration data. For the camera used here, lens distortion is extremely low, and the perspective camera is well represented by a simple pinhole imaging model. The principal distance for this model was known and available from prior work.
3) Specify a geometric surface (the rectification screen) on which to generate a rectified image. For this test, a simple cylindrical surface is utilized. The cylinder is assumed to have an axis that is vertical in the three-dimensional (3D) reconstruction coordinate system.
4) Exterior attitude alignment for the ball/camera combination (relative to the 3D reconstruction coordinate frame in which the rectification screen is defined) is determined by:
   a) Identify (manually) image point (row/column) locations for two or more points in reflection, that correspond points that are desired to be on the horizon.
   b) These image points are used in an inverse ray trace (ref appendix B) to compute a collection of object space rays emanating from the sphere. Provided the image points are correctly identified (and exterior geometry configuration is correct), then these rays are expected to be nominally coplanar with each other.

c) Compute the 3D rotation that best aligns (in least squares sense) the inverse horizon rays with the known horizontal direction in the reconstruction frame.
d) For this simple experiment, the location of the ball is (arbitrarily) set to be at the origin of the reconstruction frame.
e) Overall, the this provides a complete exterior orientation for the overall catadioptric system (expressed with respect to the reconstruction frame in which the virtual cylindrical screen is defined)

2) Rectified Image Rendering: For visualization, the solution geometry is used to synthesize an output image.

1) The object space surface (here the cylinder described above) is associated with a rectification "screen" that is partitioned into a grid of row/column cells. Each screen cell location is associated with a single pixel cell in the output image (i.e. the pixel locations associated with image in figure 6).
2) The rectification process involves performing the following computations for *each* screen (output) pixel[5].
   a) Use screen pixel (row/column) location to assign a world location, p.
   b) Apply the solution recipe from section II-B5 to determine the reflection point location, r, located on the sphere surface.
   c) Transform the representation of location, r, from expression in the reconstruction frame (cylinder frame) into expression in the catadioptric system frame.
   d) Apply the camera calibration model to determine the sensor detector location on which the image of point r is formed.
   e) Use the detector location to retrieve the corresponding image pixel value (i.e. RGB color numbers) from the source image (ref figure 5). For this experiment, a simple nearest-neighbor selection of radiometric value was used[6].

C. Rectified Image

The process described section III-B above was implemented in a computer program. Using this program, the source image shown in figure 5 was transformed into the (cylindrically) rectified output image shown in figure 6.

D. Analysis

The experiment was performed only as a general check on the formulae and relationships presented herein. A number of approximations and simplifications affect the results in addition to theoretical limitations associated drop of available information at the edge of and behind the sphere. Several of these effects as well as residual errors and artifacts are identified by annotations in figure 7.

[5]In general, the geometry computations can be performed for a sparse distribution of pixel locations, and those geometric results then interpolated for use to assign locations for intervening pixel. However, for this experiment, no interpolation optimizations were performed and the full geometric computations were performed exactly for each and every pixel.

[6]Nearest-neighbor radiometric assignment methods can produce anti-aliasing artifacts colloquially known as "the jaggies". However, the nearest neighbor radiometric assignment is often better for assessing geometric processing quality which is the objective herein.

Figure 6. Cylindrically rectified image generated from the source image shown in figure 5. The geometry of this image is generated using a vertical cylinder centered on the sphere. Rows of image pixels correspond to constant elevation value along this cylinder, while columns of images correspond to constant azimuth direction.

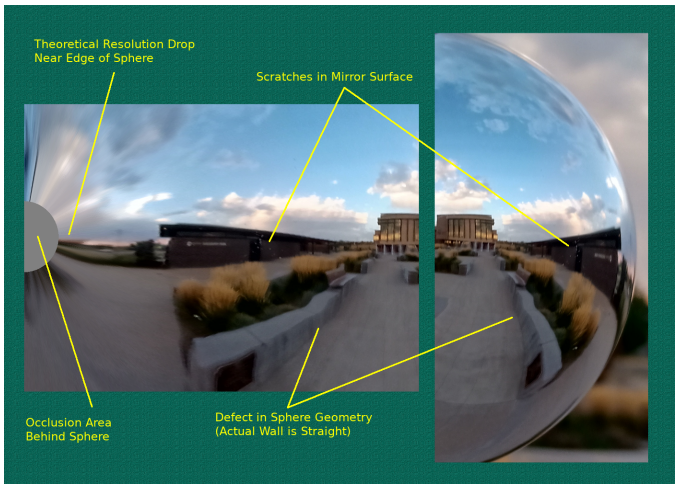

Figure 7. Identification of residual artifacts associated with various idealizations and approximations involved in this simple demonstration exercise. Several effects are identified by the annotation in the imagery.

E. Performance

1) Precision/Convergence: The iterative update formula described in section II-B3 is based on a linear approximation of the reflection condition. For comparison, a second order update formula is developed and described in appendix A. However, in practice, the linear update is found to converge sufficiently quickly (quadratically when near the solution root). Using the second order formula can improve the rate of convergence slightly. However it also introduces a spurious candidate update value which needs to be considered and complicates the process. Also, the second order update values can diverge more easily than do the linear updates. Overall, use of the simple linear-update iteration scheme seems most generally practical.

F. Speed

For this single image experiment, no effort (whatsoever) was made to improve, much less to optimize, the computation process.

Table I
PERFORMANCE RELATED INFORMATION

Item	Values
Output Image Size	975 (rows) by 3064 (columns): 3 MPix
Input Image Size	4160 (rows) by 3120 (columns): 13 MPix
Processor (one core only)	AMD Ryzen 7 2700
Time (including I/O)	2.6 sec
Time (processing only)	2.1 sec

The formula were implemented as a direct translation of the equations as presented herein, and often repeating computation of values used more than once. Computations are done using general purpose Geometric Algebra operations with no attempt to exploit computational sparsity associated with the two-dimensional reflection plane computations.

Also geometry computations are performed *in-full* for *every* individual output pixel (e.g. *no* caching of repeated/reused intermediate results, and *no* interpolation models). For practical application work, the amount of computation generally can be reduced by orders of magnitude without appreciably affecting visual results.

Several data items relative to computation timing performance (with emphasis on the sub-optimal conditions described) are presented in table I.

IV. CONCLUSIONS

The results confirm that the developed formulae and solution technique are valid for practical use.

REFERENCES

[1] University of Cambridge, "Geometric Algebra", Website, http://geometry.mrao.cam.ac.uk/
[2] Hestenes, David, "New Foundations for Classical Mechanics", Kluwer Academic Press, 1999.

APPENDIX

A. Second Order Update

A second order approximating expression for bivector-valued function, F,

$$F(\alpha) = \left\langle Ae^{2\alpha I} + Be^{\alpha I} + \gamma \right\rangle_2$$

may be expressed as,

$$\left[F(\alpha) \simeq F(\alpha_0) + \left.\frac{\partial F}{\partial \alpha}\right|_0 (\alpha - \alpha_0) + \left.\frac{\partial^2 F}{\partial \alpha^2}\right|_0 (\alpha - \alpha_0)^2 \right] = 0$$

Denote the first order bivector derivative as D, and the second order one as S, i.e.

$$\begin{aligned} F_0 &\equiv F(\alpha_0) = \left\langle Ae^{2\alpha I} + Be^{\alpha I} + \gamma \right\rangle_2 \\ D &\equiv \left.\frac{\partial F}{\partial \alpha}\right|_0 = \left\langle 2Ae^{2\alpha I} I + Be^{\alpha I} I \right\rangle_2 \\ S &\equiv \left.\frac{\partial^2 F}{\partial \alpha^2}\right|_0 = -\left\langle 4Ae^{2\alpha I} + Be^{\alpha I} \right\rangle_2 \end{aligned}$$

and define scalar difference value, δ, as

$$\delta \equiv \alpha - \alpha_0$$

In terms of these values, the approximation expression is

$$F_0 + D\delta + S\delta^2 \simeq 0$$

To put in standard form, multiply from the left by S^{-1} to obtain,

$$\delta^2 + S^{-1}D\delta + S^{-1}F_0$$

Since all the spinors are associated with parallel planes, their pairwise products reduce to scalar values, and this is a classic scalar-valued quadratic equation.

Introduce scalar values, μ and ν, defined as

$$\begin{aligned} \mu &\equiv \frac{1}{2} S^{-1} D \\ \nu^2 &\equiv S^{-1} F_0 \end{aligned}$$

Express the quadratic as

$$\delta^2 + 2\mu\delta + \nu^2 = 0$$

for which the solutions are

$$\delta = -\mu \pm \sqrt{\mu^2 + \nu^2}$$

Given a current estimate, α_n, an improved estimate of the root, based on second order approximation, is

$$\alpha_{n+1} = \alpha_n + \delta$$

B. Inverse Direction Ray Trace

Determination of the ray geometry associated with a known image pixel is relatively straight forward (provided that the perspective camera geometry is well characterized, as is assumed here).

With reference to figure 2, the known image pixel (and camera configuration data) effectively determine the direction of the reflected ray, $\hat{v}$. Let the scalar parameter, λ, represent the (unknown) range from the camera to the point of reflection on the sphere, so that $v = \lambda\hat{v}$. The camera station, point of reflection and the center of the sphere form a triangle. The geometric closure of this triangle may be expressed as the vector relationship,

$$t - v - r = 0 \tag{19}$$

Transpose r to the right hand side, and square to obtain,

$$(t - v)^2 = r^2 = \rho^2$$

Expand the left side

$$\begin{aligned} (t - v)^2 &= t^2 - 2t \cdot v + v^2 \\ &= t^2 - 2(t \cdot \hat{v})\lambda + \lambda^2 \end{aligned}$$

And combine to obtain a scalar quadratic equation in standard form,

$$\lambda^2 + 2(-t \cdot \hat{v})\lambda + \left(t^2 - \rho^2\right) = 0$$

The solutions for the range parameter (when they exist) are

$$\lambda_\pm = (t \cdot \hat{v}) \pm \sqrt{(t \cdot \hat{v})^2 - (t^2 - \rho^2)}$$

A negative value for the radicand corresponds to the case in which the ray incident into the perspective camera has missed

the sphere - i.e. has traveled from point p to point t without reflection (in which case $p = -v$).

For rays reflected from the convex outside of the sphere, the smaller root value represents the point of reflection close to the camera (i.e. λ_-), while the larger range value (i.e. λ_+) is relevant for reflection from the concave inside of the sphere.

Given a solution for the range distance, λ, the reflection point on the sphere at, r, is fully specified by rearrangement of above relationship 19 expressed as,

$$r = t - \lambda\hat{v}$$

The incident ray direction, $\hat{u}$, is determined by inverting the relationship in equation 5

$$\hat{u} = -r^{-1}\hat{v}r$$

The object location must be located somewhere along the (reversed) direction of the incident ray. Introducing scalar value, μ, as a free parameter, the object point position, p, can be expressed as

$$p = r - \mu\hat{u}$$

The negative sign arises here, since $+\hat{u}$ is defined as the direction of the forward ray propagation (cf. figure 2).

In terms of observed direction, $\hat{v}$, and solution vector, r, the point location, in terms of free parameter, μ, may be expressed as,

$$p = r + \mu r^{-1}\hat{v}r$$

For positive values $0 < \mu$, this describes a geometric ray starting at the reflection point on the sphere and propagating in a straight line toward the object point which is at an arbitrary distance, μ. A specific value for the distance to the object point, $|p - r| = \mu$, is not determined by a single image[7].

[7]A conventional imaging camera system records only direction information while range information is lost in the image acquisition process. This "collapse" of range information happens independent of any individual ray reflections. However, if there are multiple reflective objects in the scene, then multiple rays may be generated from different pixel locations within the same perspective image and these multiple rays may be used to determine a full 3D description of point, p. In such a case, the multiple reflective objects effectively create a stereo-metric, multi-mirror camera configuration. However, for the simple case of one camera and one sphere as addressed here, object range information can not readily be recovered.